Insights into the dielectric response of ferroelectric relaxors from statistical modeling

J. Liu, F. Li, Y. Zeng, Z. Jiang, L. Liu, D. Wang, Z.-G. Ye, and C.-L. Jia

Phys. Rev. B **96**, 054115 — Published 22 August 2017

DOI: 10.1103/PhysRevB.96.054115

Insights into dielectric response of ferroelectric relaxors by statistical modeling

J. Liu,[1] F. Li,[2] Y. Zeng,[3] Z. Jiang,[4,5] L. Liu,[6] D. Wang,[4,*] Z.-G. Ye,[7,2] and C.-L. Jia[4,8]

[1]*State Key Laboratory for Mechanical Behavior of Materials, School of Materials Science and Engineering, Xi'an Jiaotong University, Xi'an, China, 710049*
[2]*Electronic Materials Research Laboratory-Key Laboratory of the Ministry of Education and International Center for Dielectric Research, Xi'an Jiaotong University, Xi'an 710049, China*
[3]*School of Materials Science and Engineering, State Key Laboratory of New Ceramics and Fine Processing, Tsinghua University, No.1, Qinghua Yuan, Beijing, 100084, China*
[4]*School of Electronic and Information Engineering & State Key Laboratory for Mechanical Behavior of Materials, Xi'an Jiaotong University, Xi'an 710049, China*
[5]*Physics Department and Institute for Nanoscience and Engineering, University of Arkansas, Fayetteville, Arkansas 72701, USA*
[6]*College of Materials Science and Engineering, Guilin Univeristy of Techonology, Guilin, 541004, China*
[7]*Department of Chemistry and 4D LABS, Simon Fraser University, Burnaby, British Columbia, Canada V5A 1A6*
[8]*Peter Grünberg Institute and Ernst Ruska Center for Microscopy and Spectroscopy with Electrons, Research Center Jülich, D-52425 Jülich, Germany*

(Dated: 9th June 2017)

Ferroelectric relaxors are complex materials with distinct properties. The understanding of their dielectric susceptibility, which strongly depends on both temperature and probing frequency, has been a challenge to researchers for many years. Here we report a macroscopic and phenomenological approach based on statistical modeling to investigate how the dielectric response of a relaxor depends on temperature. Employing the Maxwell-Boltzmann distribution and considering temperature dependent dipolar orientational polarizability, we propose a minimum statistical model and specific equations to understand and fit numerical and experimental dielectric responses versus temperature. We show that the proposed formula can successfully fit the dielectric response of typical relaxors, including $Ba(Zr,Ti)O_3$, $0.87Pb(Zn_{1/3}Nb_{2/3})_{0.87}O_3$-$0.13PbTiO_3$, $0.95Pb(Mg_{1/3}Nb_{2/3})O_3$-$0.05Pb(Zr_{0.53}Ti_{0.47})O_3$, and Bi-based compounds, which demonstrate the general applicability of this approach.

I. INTRODUCTION

Relaxor ferroelectrics are materials that exhibit interesting dielectric responses different from normal ferroelectrics. For instance, they often possess relaxation modes at low frequency (< 1 GHz). Relaxor ferroelectrics have been exploited in many applications such as actuators due to their giant electromechanical couplings[1,2], and their properties extensively investigated, including structural properties (e.g., polar nanoregions or PNRs) using neutron scattering[3], dielectric responses[4–9], the crossover from ferroelectrics to relaxor[9]. To understand such systems, many theories have been proposed[3,10–16]. Relaxors are complex systems, to some extent similar to spin glasses[13,14,17], in that their compositions are, without exception, made of complex oxides containing different ions and inevitably inhomogeneous. For instance, the B-site ions of typical relaxors $Ba(Zr,Ti)O_3$ (BZT) and $Pb(Mg_{1/3}Nb_{2/3})O_3$(PMN) are randomly distributed.

The dielectric response of ferroelectric relaxors is the defining feature that differentiates them from normal ferroelectrics: (i) large susceptibilities at low frequency (GHz or lower); (ii) even more unusual, the characteristic temperature T_m at which the susceptibility peaks, strongly depends on the frequency of the probing *ac* electric field. In other words, the susceptibility, χ, depends on both temperature, T, and the probing frequency, ν. While such phenomena are well known experimentally[11,18–23], numerical generation of relaxor's dielectric response from model-based simulations has been a challenging work. For instance, the shift of T_m of the lead-free relaxor BZT was only numerically simulated recently[6]. Since numerous ferroelectric relaxors exist, numerically treating each of them remains a daunting task. One way to mitigate this difficulty is to resort to statistical modeling[24]. For a complex system, a statistical approach can provide intuitive understanding by capturing dominant factors, derive equations to understand experimental results, and help extracting useful information. In the present work, we adopt this approach to treat the dielectric response of relaxors and show that such a statistical model can indeed be applied to understanding how the dielectric constants change with temperatures and probing frequency.

While the susceptibility of relaxors, $\chi(T,\nu)$, depends on both temperature and frequency, theoretical models are often proposed to treat ν and T separately[7,10,11,25–27]. For instance, at a given temperature, two processes are employed in the fitting of $\chi(\nu)$ of Ba $(Ti_{0.675}Zr_{0.325})O_3$[18,22]: the universal relaxor process and the conventional relaxor process, which have different relaxation characteristics employing the Curie-von Schweidler law at low frequency and the Kohlrausch-Williams-Watts law at higher frequency[18]. Other formula, such as the Cole-Cole and the Havriliak-Negami equations, are also employed to model the dielectric response with respect to frequency at given temperatures. When phonon modes are close to or interacting with the relaxation modes, it becomes necessary to use coupled modes to model the dielectric response[5,6]. On the other hand, there are also many investigations on how the dielectric response, χ, depends on the temperature, T, at given frequencies. In addition to the well known Curie law for $\chi(T)$ at high temperature, most useful equation for fitting around the dielectric peak appears to be the square law. In

particular, the formula

$$\frac{1}{\varepsilon(T)} = \frac{1}{\varepsilon_A} + \frac{(T-T_A)^{\eta}}{B} \tag{1}$$

was proposed to describe the permittivity at $T > T_m$[28,29]. Initially, η was found to be 2, but later was shown to be between 1 and 2[4,11,30–32]. Here, we further the investigation in this direction and attempt to address some important questions regarding relaxor behaviors. We will explain why the dielectric constant has a peak value at T_m, and what causes the asymmetry around the peak. Moreover, by constructing a statistical model that properly describes how dipoles behave in relaxors, we propose formula to fit experimental results, which further illuminates the physics behind relaxation behavior.

This paper is organized as follows. In Sec. II, we introduce the statistical model. In Sec. III, we apply this model to both lead-free and lead-based relaxors. In Sec. IV, we discuss the implication and limitation of this approach. Finally, in Sec. V, we present a brief conclusion.

II. STATISTICAL MODEL

The statistical model starts by considering a critical difference between ferroelectric relaxors and normal ferroelectrics. One crucial observation is that all relaxor ferroelectrics discovered so far are inevitably disordered and inhomogeneous systems. For instance, in BZT, Zr and Ti ions are distributed randomly, so are the Mg and Nb ions in PMN, when the samples are treated macroscopically. In addition, PMN possesses the electric field arising from heterovalent Mg^{2+} and Nb^{5+} ions, which affects dipole distribution. It is important to further note that well known relaxors can become non-relaxor if their ions are perfectly ordered[33–35].

A. Individual dipoles

The randomness of ions and the ensuing lack of long-range ordering has the important consequence that phonon modes may not be the best description to understand relaxor. This fact is evidenced by the effective Hamiltonian that describes the BZT relaxor[12–14]

$$E = \sum_i \left(\kappa_i |u_i|^2 + \lambda_i |u_i|^4 \right) + \ldots, \tag{2}$$

where i labels the sites occupied randomly by Zr or Ti, and κ_i (λ_i) are the second (fourth) order coefficients in the Taylor expansion of energy with respect to $\mathbf{u}_i$, which is the local dipole on site i. For a homogeneous system, where k_i and λ_i are constants, we can usually first consider the harmonic term and construct phonon modes, which are then used to describe the system, especially in low temperature when the system condenses to particular phonon modes[36]. In contrast, with the loss of periodicity in relaxors, this approach is no longer profitable. One can insist on using averaged atoms (e.g., replacing Zr and Ti atoms with their average in BZT) to retain the use of phonon modes. However, it is then necessary to consider defect-pinned intrinsic localized modes[37] and phonon localization[3].

The inhomogeneity also has important consequences on ferroelectric phase transitions. In the typical ferroelectric material $BaTiO_3$, we may ascribe the temperature-driven phase transition to the condensation of phonons to a particular phonon mode[36]. At high temperature, many phonons modes are occupied; at low temperatures, due to mode softening, certain mode (often corresponding to the well-known soft mode[38–40] in perovskites) has essentially zero energy, which dominates the system and induce phase transitions. Unlike $BaTiO_3$, there is no global phase transition due to the existence of PNRs and/or random electric fields, which eliminates the mode softening phenomenon and renders a global dipole order difficult to achieve[12,41]. In addition, relaxors exhibit strange phonon behavior, such as the "waterfall" effect[42–44] and the localization[3], further showing their difference from normal ferroelectrics. In this work, we focus on individual dipoles and statistically model their dielectric response. This change of view implies that phonon modes are less important in our analysis. We will show in the following that such consideration leads to fruitful results, and better understanding of relaxors.

B. Statistics of individual dipoles

Individual dipoles can be categorized into different groups based on their dynamics, and each group shall have different contribution to susceptibility. We proceed by summarizing various interactions between dipoles and assuming such interactions effectively introduce a potential well of *average* depth, E_b. We may relate E_b to the size of PNRs arising from the clustering of the same-type ions[12] and/or random electric field caused by heterovalent ions[41,42,45].

Since the kinetic energy of individual dipoles obeys the Maxwell-Boltzmann distribution, at temperature T, the number of dipoles with kinetic energy E_{kin} is given by

$$f(E_{\text{kin}}) = 2N\sqrt{\frac{E_{\text{kin}}}{\pi}} \left(\frac{1}{k_B T}\right)^{3/2} \exp\left(-\frac{E_{\text{kin}}}{k_B T}\right), \tag{3}$$

where k_B is the Boltzmann constant, N is the total number of dipoles, and $f(E_{\text{kin}})\,dE_{\text{kin}}$ is the number of dipoles having a kinetic energy between E_{kin} and $E_{\text{kin}} + dE_{\text{kin}}$. With this distribution function, we can calculate the number of dipoles with kinetic energy that exceeds the potential well E_b, which is given by

$$\begin{aligned} N_1(E_b, T) &= \int_{E_b}^{\infty} dE_{\text{kin}} f(E_{\text{kin}}) \\ &= N\sqrt{\frac{4}{\pi}}\sqrt{\frac{E_b}{k_B T}} \exp\left(-\frac{E_b}{k_B T}\right) + N\,\text{erfc}\left(\sqrt{\frac{E_b}{k_B T}}\right), \end{aligned} \tag{4}$$

where erfc is the complementary error function. The number of dipoles confined to the potential well is then given by

$$N_2(E_b, T) = N - N_1(E_b, T). \tag{5}$$

The next step is to treat the two sets of dipoles (N_1 versus N_2) separately, assigning different susceptibility to them. The total susceptibility is then given by

$$\chi(T,\nu) = \chi_1(T,\nu) P_1(E_b,T) + \chi_2(T,\nu) P_2(E_b,T), \quad (6)$$

where $\chi_1(T,\nu)$ and $\chi_2(T,\nu)$ describe the dielectric responses of each dipole group, whose form will be specified later. We also define

$$P_1(E_b,T) \equiv \frac{1}{N} N_1(E_b,T),$$
$$P_2(E_b,T) \equiv \frac{1}{N} N_2(E_b,T),$$

to normalize the dipoles to unit volume. Equation (6) is the centerpiece of this work and will be demonstrated to be useful for the investigation of relaxors in general.

III. RESULTS

We apply Eq. (6) to fit various χ versus T obtained experimentally or numerically. The relaxors studied here include both lead-basd (e.g., PMN) and lead-free relaxors (e.g., BZT).

A. Susceptibility of BZT

For the static susceptibility of lead-free relaxor BZT[6,8,22,46], we assume (i) dipoles with kinetic energy that overcomes potential well can be treated as free dipoles, subject only to thermal excitation; (ii) dipoles inside the potential well only contribute a constant susceptibility, χ_2. The total susceptibility is thus given by

$$\chi(T) = \chi_1 \mathscr{L}\left(\frac{\theta}{T}\right) P_1(E_b,T) + \chi_2 P_2(E_b,T), \quad (7)$$

where $\mathscr{L}(x) = \coth(x) - 1/x$ is the Langevin function, known for depicting orientational polarization under thermal fluctuations[47,48], and E_b, χ_1, χ_2 and θ are constants which will be determined by fitting experimental or numerical data. It can be inferred from equation (7) that χ_1 is the susceptibility of the material at zero Kevin, $\chi_1 \mathscr{L}\left(\frac{\theta}{T}\right)$ is essentially the Curie law at high temperatures, and θ is proportional to the magnitude of the low-frequency electric field used in experimental measurements.

We first test Eq. (7) against the static susceptibility versus temperature obtained with Monte-Carlo (MC) simulation in a previous work[12]. Figure 1 shows that the overall fitting is good enough to reproduce results from MC simulations with parameters shown in Tab. I. The closeness of E_b and T_m indicates the average depth of potential wells plays a dominant role in determining T_m. Close examination of Fig. 1 also reveals that the fitting at the lowest temperature ($\lesssim 25$ K) is not as good as the rest. To address this issue, we added a Gaussian distribution to E_b to remedy this minor problem. However, the resulting equation is quite complicated and deviates from our original goal of proposing simple analytical formula to fit susceptibility. Therefore this additional step is not adopted here.

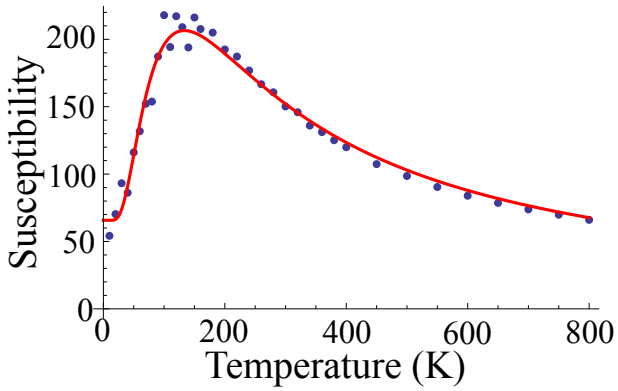

Figure 1: Fitting the static susceptibility of $Ba(Zr_{0.5},Ti_{0.5})O_3$ obtained from Monte-Carlo simulation using Eq. (7). The blue dots are from Monte-Carlo simulation[12] and the red solid line is the fitting curve using Eq. (7).

	χ_1	θ (K)	χ_2	E_b (K)
Values	741.6	220.5	64.7	159.1

Table I: Fitting parameters for the $Ba(Zr_{0.5},Ti_{0.5})O_3$ static susceptibility.

In order to have a good understanding of BZT's susceptibility, we show each component of Eq. (7) in Fig. 2. Figure 2 (a) shows that $P_1(E_b,T)$ and $P_2(E_b,T)$ have opposite trends as temperature increases. The number of dipoles that can overcome the potential confinement (P_1) steadily increases with temperature, while the number of dipoles inside (P_2) continuously becomes smaller. Figure 2 (b) shows that the Lagevin function is normalized at $T = 0$, and decreases with temperature. Such a feature describes the ability of the free dipoles to respond to an external *dc* electric field. Moreover, Fig. 2 (b) also shows the product of the Langevin function and P_1, which already exhibits some resemblance to the BZT's susceptibility [Fig. (1)].

Having examined the static susceptibility, we now move to the frequency-dependent dielectric response, which is often taken as a characteristic property of relaxors[9,49]. We propose another equation to fit the susceptibility versus temperature:

$$\chi(T) = \frac{\chi_1}{1 + b\exp(-\theta/T)} P_1(E_b,T) + \chi_2 P_2(E_b,T), \quad (8)$$

where χ_1 , χ_2, b and θ are constants at a given frequency (but may change when the frequency changes). The dielectric contribution from dipoles with kinetic energy higher than the potential well is given by

$$w_1(T) = \frac{1}{1 + b\exp(-\theta/T)}. \quad (9)$$

which, similar to the Langevin function, monotonically decreases with temperature T. The choice of this function reflects

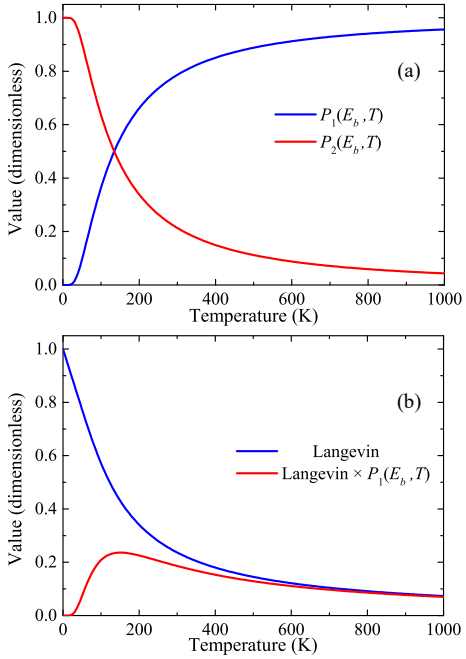

Figure 2: Maxwell-Boltzmann distribution [Panel (a)] and the Langevin function, $\mathscr{L}$, [Panel (b)] versus temperature. Parameters from Tab. I are used to plot each function.

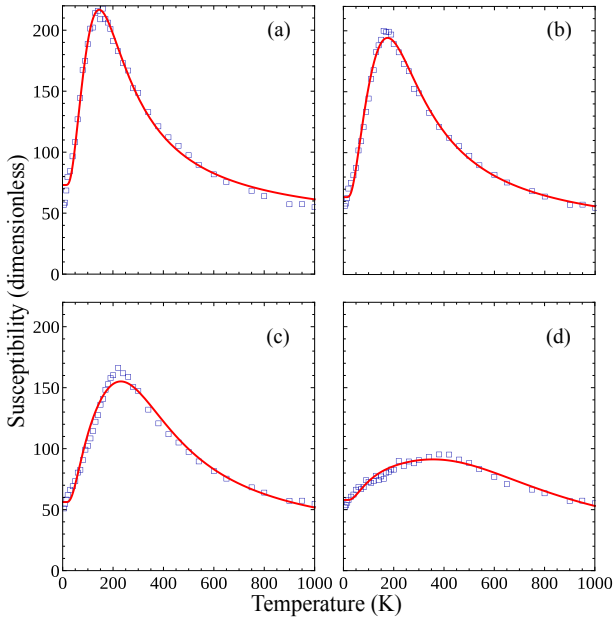

Figure 3: Fitting of the susceptibility of $Ba(Zr_{0.5},Ti_{0.5})O_3$ at $f = 1, 10, 100, 1000$ GHz, obtained from molecular dynamics simulation using Eq. (8).

two considerations: (i) at very low temperatures (T close to 0), such dipoles shall follow the probing *ac* electric field closely, leading $w_1(T)$ to its maximum; and (ii) at higher temperatures, thermal motions of these dipoles hamper their ability to follow the *ac* electric field, leading to smaller $w_1(T)$. We will discuss this equation further in Sec. IV. With one more parameter (b), this function may be taken as an extension to the Langevin function. We note that Eq. (7) can no longer be used because the Langevin function is derived under the equilibrium condition of dipoles, whereas dipoles under *ac* electric fields are never in true equilibrium, therefore invalidating the use of the Langevin function.

	1 GHz	10 GHz	100 GHz	1000 GHz
θ (K)	579.6	762.6	1128.4	2158
χ_1	406.5	312.6	209.3	99.9
χ_2	73.1	63.5	56.2	57.9
b	10.2	9.9	9.5	7.7

Table II: Fitting parameters of numerically simulated $Ba(Zr_{0.5},Ti_{0.5})O_3$ susceptibility at various frequency[6] using Eq. (8).

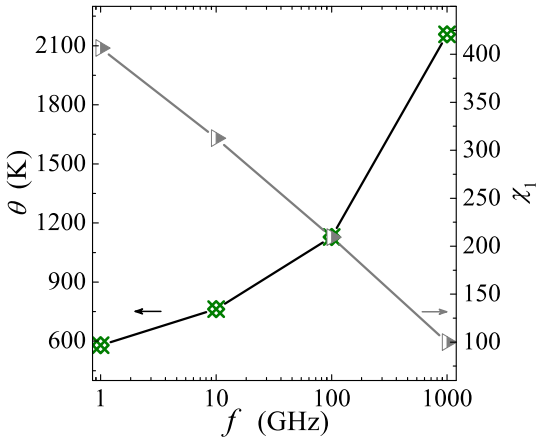

Figure 4: Analysis of fitting parameters versus probing frequency. (a) θ vs $\log(f)$ and χ_1 vs $\log(f)$.

We use Eq. (8) to fit BZT's susceptibility versus temperature at different frequencies and show the results in Fig. 3. Since E_b is a material parameter, we use the same value ($E_b = 159.1$ K) obtained by fitting the static susceptibility (cf. Fig. 1). In Fig. 3, the numerical results are obtained from molecular dynamics simulations reported in Ref. 6. As the figure shows, satisfactory fittings are achieved for frequencies between 1 and 1000 GHz. Table II shows all the parameters. Among them, θ_1 and χ_1 change substantially over the specified frequency range as shown in Fig. 4, where θ depends on $\log(f)$ quadratically, while χ_1 linearly depends on it[50].

To further verify the suitability of this equation for experimental data, we also fit the result shown in Fig. 1 of Ref. 18, where $Ba(Ti_{0.675}Zr_{0.325})O_3$ ceramics is measured at 10^{-2} and 10^5 Hz. Figure 5 shows that satisfactory fittings are achieved.

B. Pb-based relaxors

Unlike lead-free BZT, which possesses PNRs that are separated by Zr-rich regions, lead-based ferroelectrics[19,29,41,51]

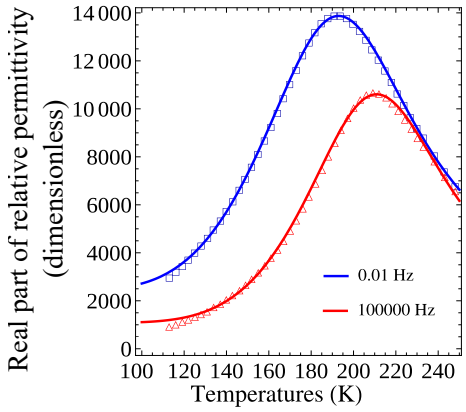

Figure 5: Experimental susceptibility of $Ba(Ti_{0.675}Zr_{0.325})O_3$ ceramics versus temperature fitted with Eq. (8).

have the Pb-driven dipoles across the system[52], which causes phase transitions in systems such as $PbTiO_3$ and $Pb(Zr,Ti)O_3$[53–55]. Due to heterovalent ions inside, typical lead-based relaxors are subject to random electric fields, which distort the orientation of dipoles. While the precise consequence of the random field is not all clear[14,15], such distracting effect on dipoles appears to lead to a strongly modified phase transition with diffuse and smeared susceptibility peak, in sharp contrast to that of normal ferroelectrics[41,56].

To model such a system and account for the moderate phase transition, we need a function that properly describes the dielectric constant versus temperature. Here, we propose to use the slightly modified well known quadratic relation $\frac{\varepsilon_A}{\varepsilon'}-1=\frac{(T-T_A)^2}{2\delta^2}$ proposed by Bokov and Ye[4] to relate relaxor's permittivity to temperature[28,29] for dipoles above the average potential well (also see Eq. (1)). This equation can be rearranged to give the following expression

$$w_2(T)=\frac{1}{1+\left|\frac{T-T_O}{\theta}\right|^{\gamma}}, \tag{10}$$

where γ is a critical exponent, T_o is associated with the peak position of the moderate phase transition, and θ is a parameter describing the width of the peak. We note that compared to $\frac{\varepsilon_A}{\varepsilon'}-1=\frac{(T-T_A)^2}{2\delta^2}$, we have used T_O instead T_A, θ instead of $\sqrt{2}\delta$, and a general critical exponent γ instead of the fixed number 2. Seciton A provides a further discussion of this formula. We also note that such choice of $w_2(T)$ also agrees with the analysis recently given by Uchino[10], who provides a possible physical interpretation to this formula. Combining Eqs. (6) and (10), we obtain the following equation to fit lead-based relaxors,

$$\chi(T)=\frac{\chi_1}{1+\left|\frac{T-T_O}{\theta}\right|^{\gamma}}P_1(E_b,T)+\chi_2 P_2(E_b,T), \tag{11}$$

where E_b, χ_1, χ_2, T_o, θ, and γ are fitting parameters. The meaning of χ_1, χ_2, and E_b are the same as discussed in Sec. III A.

Two considerations motivate the adoption of Eq. (11): (i) Pb-based relaxors usually have Pb driven dipoles that exist across the system, unlike BZT where dipole clusters (PNRs) are separated by Zr-rich regions; (ii) As a consequence of (i), despite strong random electric fields, there could be a global phase transition which exhibits temperature dependence following Eq. (10)[10].

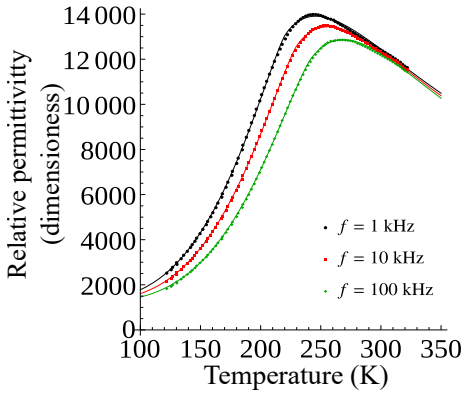

Figure 6: Fitting the relative permittivity of PZN-0.13PT at $f=1,10,100$ kHz using Eq. (11).

To verify that Eq. (11) indeed works, we experimentally obtained the permittivity of $0.87Pb(Zn_{1/3}Nb_{2/3})_{0.87}O_3$-$0.13PbTiO_3$ (PZN-0.13PT)[57,58] versus temperature at frequencies $f=1,10$ and 100 kHz[59]. As Fig. 6 shows, all three fittings are satisfactory. We note that in this fitting there is no need to have two γ values above and below T_o[10]. The asymmetric peak shown in Fig. 6 is naturally caused by the Maxwell-Boltzmann distribution function.

	1 kHz	10 kHz	100 kHz
γ	2.02	1.82	1.63
T_O (K)	219.6	229.0	240.6
E_b (K)	495.3	523.6	552.2
χ_1 [a]	56601	55781	53529
χ_2	1320.9	1284.2	1238.0
θ (K)	102.4	103.1	104.5

[a] Here, χ_1 and χ_2 are relative permittivity, not susceptibility.

Table III: Fitting parameters of PZN-0.13PT's permittivity measured at different frequencies. As the table demonstrates, γ and T_O are the most important variables that change a lot with frequency.

Table III summarizes the fitting parameters of the permittivity measured at various frequencies. Among all the parameters, the critical component γ changes the most (by 19.3% from 1 kHz to 100 kHz), and decreases with increasing frequency; similarly, T_O also changes by 9.5%. On the other hand, χ_1, χ_2, θ are relatively constant, which are independent of the frequency, and may be taken as material parameters. Such results hints towards the following formula that describes the dependence of PZN-0.13PT on both temperature and the probing

frequency:

$$\chi(T,\nu) = \frac{\chi_1}{1+\left|\frac{T-T_O(\nu)}{\theta}\right|^{\gamma(\nu)}} P_1(E_b,T) + \chi_2 P_2(E_b,T), \quad (12)$$

where the two functions $T_O(\nu)$ and $\gamma(\nu)$ are frequency dependent while other parameters are constants for a given material. It is also worth noting that for 0.87PZN-0.13PT $\chi_2 \ll \chi_1$, which indicates that the dipoles with kinetic energy above the potential well plays a more important role, in contrast to the case of BZT (see Tab. II).

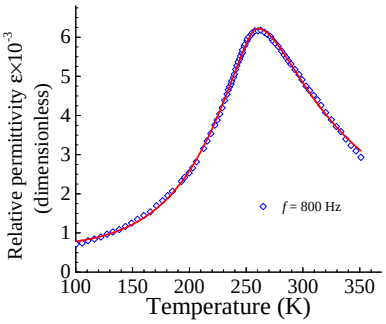

Figure 7: Fitting of the relative permittivity of $0.95Pb(Mg_{1/3}Nb_{2/3})O_3$-$0.05Pb(Zr_{0.53}Ti_{0.47})O_3$ measured at 800 Hz using Eq. (11).

To further verify the proposed formula, we also fit the permittivity versus temperature of another lead-based relaxor, $0.95Pb(Mg_{1/3}Nb_{2/3})O_3$-$0.05Pb(Zr_{0.53}Ti_{0.47})O_3$[19]. It can be seen from Fig. 7 that the overall fitting is satisfactory, with fitting parameters $\gamma = 1.66$ and $T_O = 256.7$ K. Similar to the PZN-0.13PT case, the results here also show $\chi_2 \ll \chi_1$.

IV. DISCUSSION

In the statistical model we divide the dipoles inside ferroelectrics relaxors into two groups, one group being confined in potential wells, while the other having overcome the potential confinement and exhibiting a more vibrant dynamics. It has been demonstrated that the Maxwell-Boltzmann distribution plays a significant role in determining the profile of $\chi(T)$. To address a particular type of relaxor, one only need to adjust the dielectric response function associated with each group of dipoles, while keeping the rest unchanged. In this section, we discuss a few issues of this approach and its limitations.

A. Characteristic temperature T_m

The present analysis helps us to understand why the susceptibility of a relaxor reaches its peak value at some temperature, T_m. For BZT, the function $\chi_1 \mathscr{L}\left(\frac{\theta}{T}\right)$ [see Eq. (7) and Fig. 2] or $\chi_1/[1+b\exp(-\theta/T)]$ [see Eq. (8)] describes the contribution to susceptibility from dipoles with kinetic energy higher than E_b. These two functions are both monotonically decreasing with T, reflecting the fact that thermal motions prevent dipoles from aligning with the applied electric field. On the other hand, the number of dipoles above potential wells increases with T as governed by the function $P_1(E_b,T)$ (see Fig. 2). The combined effects of the two factors give rise to the susceptibility peak at T_m. However, the situation for lead-based relaxors is different. The function $\chi_1/\left(1+\left|\frac{T-T_O}{\theta}\right|^{\gamma}\right)$ [see Eq. (11)], which largely determines the value of T_m, manifests the vestige of a true phase transition in normal ferroelectrics, which is torn down by random electric fields and/or PNRs in relaxors.

B. Rationale for Eq. (9)

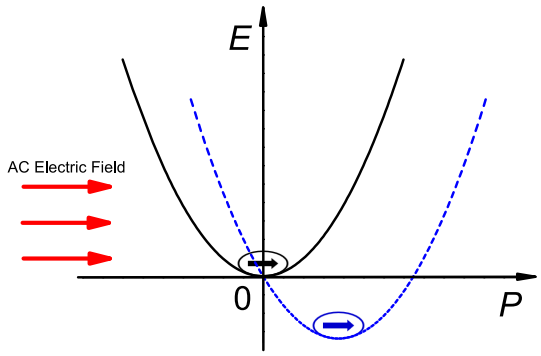

Figure 8: The energy well for dipoles is shifted and lowered when an electric field is applied .

For lead-free BZT, we propose Eq. (9) to describe the susceptibility of dipoles with kinetic energy higher than E_b. This choice follows the Debye relaxation, i.e., $\chi \sim 1/(1+\omega^2\tau^2)$[47], where ω is a constant (the probing frequency), and τ is temperature-dependent relaxation time. For a thermally activated process, the relation between τ and T is often specified by the Arrhenius law, i.e., $1/\tau = A\exp(-E_a/T)$, where $E_a > 0$ is the activation energy[37,56,60]. In this case, the susceptibility will be $\chi \sim 1/\left[1+A^2\omega^2\exp\left(\frac{2E_a}{T}\right)\right]$, which is discussed by Jonscher[61]. However, the dynamic process considered here describes dipoles falling to a state of lower energy, which is temporarily created by the probing electric field (see. Fig. 8). Therefore the activation energy in this process shall be *negative*, i.e., $\chi \sim 1/\left[1+A^2\omega^2\exp\left(-\frac{2|E_a|}{T}\right)\right]$, which is the form adopted in Eq. (9).

We note that negative activation energy is known in some chemical reactions[60]. Negative activation energy appears here because when an *ac* electric field perturbs dipoles and tilts the relative energy of potential wells, the dipoles outside potential wells will move towards the temporary potential minimum. However, the drifting to the potential minimum is hindered by thermal fluctuations of such dipoles. In fact, a higher temperature (corresponding to larger kinetic energy) results in a slower relaxation to the energy minimum (corresponding to larger τ), leading to negative activation energy. Furthermore, other interactions between dipoles (in particular short-range

interaction) may also affect this relaxation process and slow it down as temperature increases, giving rise to an apparent negative activation energy, while this is basically a zero energy barrier process. We also note that since the applied *ac* electric field is responsible for shifting the energy minimum and causing dipoles to drift, the change of its frequency may well alter the process, explaining why θ in Eq. (8) is dependent on the probing frequency. Similar arguments explain why T_O also depends on the probing frequency.

In the above analysis, we focus on dipoles with kinetic energy higher than E_b. These dipoles are able to drift from one energy minimum to another when an *ac* electric field perturbs the system. It has been proposed that the drifting/hopping of dipoles from one potential well to another causes relaxations . However, without distinguishing dipoles inside and outside the potential well, such proposal seems to have a tendency of confusing the wait time before hopping, t (which reflects the distribution of dipoles at a given temperature) with the relaxation time, τ (which reflects how fast dipoles drift to the transient energy minimum and relates to the loss peak frequency in the Debye function), leading to some difficulties.

C. Limitations

In previous studies[5,6,41], *ab initio* calculations are used, which prescribe all important interactions between dipoles and other degrees of freedom in relaxors, and then MC or MD is used to numerically work out the consequences. In the present work we do not start from *ab initio* calculation, instead, employ statistical and phenomenological arguments. Having shown results and insights obtained with this approach, we now discuss possible limitations of the present approach with respect to the treatment of details, accuracy, and prediction power.

First, the proposed equations for lead-free [Eq. (8)] and lead-based relaxors [Eq. (12)] have five and six parameters, respectively. Ideally, one hopes to be able to use as few parameters as possible. However, it shall be noted that, among these parameters, many are only material dependent (i.e., they do not depend on frequency or temperature). For instance, for lead-free relaxor, E_b is a constant; for lead-based relaxor, E_b, χ_1, χ_2 and θ are close to constants (see Tab. III). For a given sample, these parameters may only need to be calibrated once. In this way, the number of parameters will be significantly reduced.

Second, in this work we have focused on the temperature dependence of susceptibility. The dependence on frequency needs further investigation. For instance, $T_O(\nu)$ and $\gamma(\nu)$ in Eq. (12) need to be specified explicitly to address this issue. We note that the results shown in Tab. III will provide clues to the T_C and γ's dependence on ν, and eventually help finding analytical expressions for $\chi(T,\nu)$. In addition, we generally ignored possible long-range ordering of dipoles, which is another limitation to this approach. While such possible long-range ordering makes relaxor physics rich, it will bring back Bose-Einstein statistics and make the current formulation more complicated. To what extent the Bose-Einstein and the Maxwell-Boltzmann distribution shall be used for ferroelectric relaxors remains an open question.

Third, at high temperature, the Curie law is observed in many ferroelectrics. For the static susceptibility of BZT [Fig. 1], this law can be recovered from the proposed equation, Eq. (7). On the other hand, for Eqs. (8) and (11), the Curie law cannot be directly recovered. For Eq. (11), we have the asymptotic relation $\chi \sim A/(T-T_O)^\gamma + B/T^{3/2}$ at very large T. It is unclear how good this relation can fit the Curie law. Therefore, in fitting experimental data at high temperatures, one needs to bear in mind that Eqs. (8) and (11) should be used with care.

Finally, with formula such as Eq. (12),we can in principle obtain the relation between T_m and ν (assuming we know the analytical expression of $T_O(\nu)$ and $\gamma(\nu)$), which can then be compared to the well-known Vogel-Fulcher law[6]. However, we have failed to obtain analytical expressions to relate T_m (note that T_m is not T_O while they may be close) to ν and believe that numerical calculation seems to be the only feasible way to establish the relation between T_m and ν.

V. CONCLUSIONS

Instead of working on the atomic level, the present work employs a macroscopic statistical approach to describe dielectric properties of relaxors. The effects of disorder, PNRs, and random electric fields are considered statistically by introducing the average potential well, which can trap dipoles of low kinetic energy. An external electric field will mostly increase the magnitude of trapped dipoles, but can rotate dipoles free from such trapping and align them with the field. These two groups of dipoles give rise to two different types of dielectric responses as shown in Eqs. (7), (8), and (11). The analytical equations resulting from this approach provide insights to experimental and numerical results of relaxors. Among other things, it is shown that the characteristic temperature, T_m, is determined by the Maxwell-Boltzmann distribution of dipoles' kinetic energy, as well as their ability to respond to the applied electric field. We can also conclude that lead-free relaxors (e.g., BZT) are different from lead-based relaxors (e.g., 0.87PZN-0.13PT) in that (i) the mechanisms determining T_m are different. For lead-based relaxors, it appears T_O alone is able to determine T_m, while for BZT, both $w_1(T)$ and $P(E_b,T)$ are important; and (ii) for BZT, χ_1 and χ_2 are of the same order, in contrast to the fact while $\chi_1 \gg \chi_2$ for the Pb-based relaxors, indicating that the dipoles outside the average potential well dominate the dielectric response of Pb-based relaxors. These results demonstrate that this statistical approach can provide a good understanding of important relaxor systems and the proposed equations can be adopted in fitting experimental data of relaxors in general (see Sec. C).

Acknowledgments

We thank Drs C.-L. Wang, A. A.Bokov and L. Bellaiche for fruitful discussion. This work is financially supported by the National Natural Science Foundation of China (NSFC),

Grant No. 11574246, 51390472, U1537210, and National Basic Research Program of China, Grant No. 2015CB654903. F.L. acknowledges NSFC Grant No. 51572214. Z.J. acknowledges the support from China Scholarship Council (CSC No. 201506280055). L.L. acknowledges NSFC Grant No. 11564010 and the Natural Science Foundation of Guangxi (GA139008). We also acknowledge the "111 Project" of China (Grant No. B14040), the Natural Science and Engineering Council of Canada (NSERC) and the United States Office of Naval Research (ONR Grant No. N00014-12-1-1045 and N00014-16-1-3106).

Appendix A: Extended fitting range

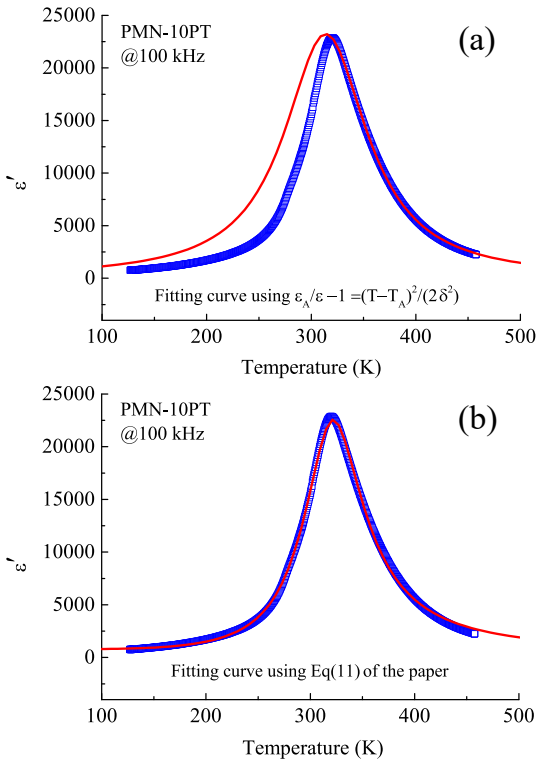

Figure 9: Fittings of the susceptibility of PMN-10PT obtained at 100 kHz are fitted with Eq. (A3) (Panel (a)) and Eq. (11) (Panel (b))

Unlike normal ferroelectrics, whose permittivity follows the well-known Curie–Weiss law $1/\varepsilon = (T - T_{CW})/C$ above the Curie temperature, relaxors obey this law only for temperatures much higher (typically hundreds of degrees) than T_m, where a broad and diffusive peak centers. Smolenskii, Kirillov and Isupov[28,29] were the first ones proposing a quantitative description of such peaks. They suggested that the total number of relaxators contributing to the dielectric response in the vicinity of the permittivity peak is temperature dependent, governed by a Gaussian function with a mean value of T_O and a standard deviation δ . With some additional assumptions, they derived the following expression:

$$\frac{\varepsilon_0}{\varepsilon - \varepsilon_\infty} = \exp\left[\frac{(T - T_o)^2}{2\delta^2}\right], \tag{A1}$$

where ε_∞ is the high-frequency contribution, and ε_0 is a temperature and frequency-dependent parameter.

Neglecting ε_∞ and assuming that T_O is equal to the temperature where permittivity peaks (T_m), one can expand Eq. (A1) and obtain a truncated power series[11]

$$\frac{\varepsilon_m}{\varepsilon} = 1 + \frac{(T - T_m)^2}{2\delta_m^2}, \tag{A2}$$

The quadratic law [Eq. (A2)] was found to be approximately valid for $T > T_m$ for many materials. However, the deviations of some experimental data from the quadratic law incited many authors to search for new formula. A power law was proposed[30,31]

$$\frac{\varepsilon_m}{\varepsilon} = 1 + \frac{|T - T_m|^\gamma}{2\delta_\gamma^2}, \tag{A3}$$

with $1 \le \gamma \le 2$, which differs from Eq. (A2) in that an empirical exponent γ is used instead of 2. This expression can be rearranged to give

$$\frac{\varepsilon}{\varepsilon_m} = \frac{1}{1 + \frac{(T-T_m)^\gamma}{2\delta_\gamma^2}} = \frac{1}{1 + \left|\frac{T-T_m}{(2\delta_\gamma^2)^{1/\gamma}}\right|^\gamma}, \tag{A4}$$

where the RHS is just the $w_2(T)$ we propose in Eq. (10).

While Eq. (A2) or (A3) can successfully fit the temperature range $T > T_m$, it is hard to fit the whole temperature range that is experimentally reachable [see Fig. 9(a)], with the main obstacle being the asymmetrical line shape around T_m. This obstacle is now resolved in this work by introducing Eq. (11), where the asymmetry is accounted for by considering the Maxwell-Boltzmann distribution of dipoles. We illustrate this point in Fig. 9 where fittings of PMN-10PT using Eq. (A3) and Eq. (11) are compared.

Appendix B: $w_1(T)$ and $w_2(T)$

Figure 10 plots $w_1(T)$ [Eq. (9)]and $w_2(T)$ [Eq. (10)]with their parameters obtained by fitting BZT (Fig. 3), PZN-0.13PT (Fig. 6), and 0.95Pb($Mg_{1/3}Nb_{2/3}$)O_3-0.05Pb($Zr_{0.53}Ti_{0.47}$)O_3 (Fig. 7).

Figure 10(a) shows that at low frequency ($\lesssim 10$ GHz), $w_1(T)$ resembles the Fermi-Dirac function, that is, below$\sim$ 250 K, its value is close to one but becomes close to zero for T above $\sim$ 250 K. At a higher frequency (e.g., 1000 GHz), however, this function strongly deviates from the Fermi-Dirac function, with a long tail extending to high temperatures. Figures 10(b) and (c) show that $w_2(T)$ is a symmetric peaks, likely related to a phase transition in lead-based relaxor. For Fig. 10(b), the peak position (around 220 K) slightly shifts toward higher temperature with increasing frequency.

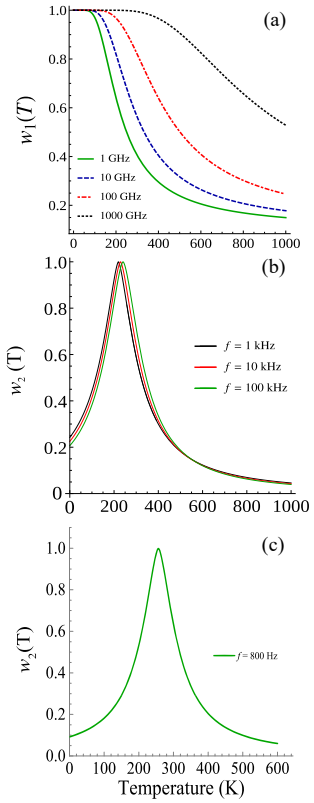

Figure 10: The plotting for $w_1(T)$, and $w_2(T)$ with their parameters obtained by fitting BZT (Panel (a), also see Fig. 3), PZN-0.13PT (Panela (b), also see Fig. 6), and 0.95Pb($Mg_{1/3}Nb_{2/3}$)O_3-0.05Pb($Zr_{0.53}Ti_{0.47}$)O_3 (Panel (c), also see Fig. 7).

Appendix C: Applicability to other systems

In previous sections, we have focused on BZT and lead based relaxor ferroelectrics and shown their fitting results. As a matter of fact, we have tested the proposed formula with various relaxor systems and obtained useful results. Figure 11 shows the results of four relaxor systems and the fitting of the real part of their permittivity: (i) PMN; (ii) PMN-10PT; (iii) 0.4($Ba_{0.8}$,$Ca_{0.2}$)$La_{0.3}TiO_3$-0.6Bi($Mg_{0.5}$,$Ti_{0.5}$)O_3; (iv) 0.55Bi($Ni_{1/2}$,$Ti_{1/2}$)O_3-0.45$PbTiO_3$. For these fittings, we have used Eq. (11) and obtained satisfactory results with fitting parameters shown in Tab. IV, which further demonstrates the applicability of our approach.

	PMN	PMN-10PT	0.4BCLT-0.6BMT	0.55BNT-0.45PT
χ_1	32201.07	67955.26	45373.38	11510.60
E_b(K)	497.99	556.61	2204.65	985.24
χ_2	442.07	792.65	271.47	232.94
T_O(K)	272.73	319.51	364.84	508.84
θ	44.10	35.71	121.38	255.20
γ	1.83	1.92	1.96	1.52

Table IV: Fitting parameters of various materials obtained using Eq. (11).

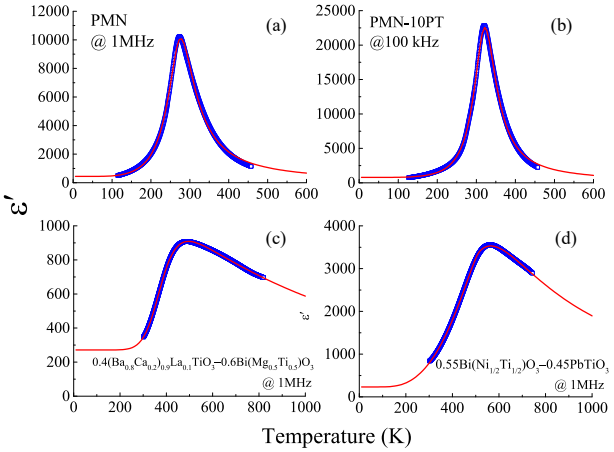

Figure 11: Fitting the permittivity of various materials using Eq. (11). The blue circles are experimental data and the red solid line is the fitting curve.

* Electronic address: dawei.wang@mail.xjtu.edu.cn

1 K. Uchino, Piezoelectric Actuators and Ultrasonic Motors. (Springer, 1996).

2 F. Li ,S. Zhang, T. Yang, Z. Xu, N. Zhang, G. Liu, J. Wang, J. Wang, J. Wang, Z. Cheng, Z. Ye, J. Luo, T. R. Shrout, and L. Cheng, The origin of ultrahigh piezoelectricity in relaxor-ferroelectric solid solution crystals. *Nat. Commun.* **7**, 13807 (2016).

3 M. E. Manley, J. W. Lynn, D. L. Abernathy, E. D. Specht, O. Delaire, A. R. Bishop, R. Sahul, and J. D. Budai, Phonon localization drives polar nanoregions in a relaxor ferroelectric. *Nat. Commun.* **5**, 3683 (2014).

4 A. A. Bokov and Z.-G. Ye, Recent progress in relaxor ferroelectrics with perovskite structure. *J. Mater. Sci.* **41**, 31 (2006).

5 D. Wang, J. Hlinka, A. A. Bokov, Z. G. Ye, P. Ondrejkovic, J. Petzelt, and L. Bellaiche. Fano resonance and dipolar relaxation in lead-free relaxors. *Nat. Commun.* **5**, 5100 (2014).

6 D. Wang, A. A. Bokov, Z.-G. Ye, J. Hlinka, and L. Bellaiche, Subterahertz dielectric relaxation in lead-free Ba(Zr,Ti)O_3 relaxor ferroelectrics. *Nat. Commun.* **7**, 11014 (2016).

7 D. Nuzhnyy, J. Petzelt, and M. Savinov, Broadband dielectric response of Ba(Zr,Ti)O_3 ceramics: from incipient via relaxor and diffuse up to classical ferroelectric behavior. *Phys. Rev. B* **86**, 014106 (2012).

8 J. Petzelt, D. Nuzhnyy, M. Savinov, V. Bovtun, M. Kempa, T. Ostapchuk, J. Hlinka, G. Canu, and V. Buscaglia, Broadband dielectric spectroscopy of Ba(Zr,Ti)O_3: dynamics of relaxors and diffuse ferroelectrics. *Ferroelectrics* **469**, 14 (2014).

9 W. Kleemann, S. Miga, Z. K. Xu, S. G. Lu, and J. Dec, Non-linear permittivity study of the crossover from ferroelectric to relaxor and cluster glass in $BaTi_{1-x}Sn_xO_3$. *Appl. Phys. Lett.* **104**, 182910 (2014).

10 K. Uchino, Fractal Phenomena in Ferroelectrics. *J. Nanotech.*

Mater. Sci. **1**, 1 (2014).
[11] A. A. Bokov and Z.-G. Ye, Dielectric relaxation in relaxor ferroelectrics. *J. Adv. Dielectr.* **2**, 1241010 (2012).
[12] A. Akbarzadeh, S. Prosandeev, E. Walter, A. Al-Barakaty, and L. Bellaiche, Finite-temperature properties of Ba(Zr, Ti)O_3 relaxors from first principles. *Phys. Rev. Lett.* **108**, 257601 (2012).
[13] D. Sherrington, BZT: a soft pseudospin glass. *Phys. Rev. Lett.* **111**, 227601 (2013).
[14] D. Sherrington, Pb($Mg_{1/3}Nb_{2/3}$)O_3: A minimal induced-moment soft pseudospin glass perspective. *Phys. Rev. B* **89**, 064105 (2014).
[15] W. Kleemann, J. Dec, and S. Miga, The cluster glass route of relaxor ferroelectrics, *Phase Trans.* **88**, 234 (2015).
[16] R. Pirc, R. Blinc, Spherical random-bond-random-field model of relaxor ferroelectrics. *Phys. Rev. B* **60**, 13470 (1999).
[17] D. Sherrington, A spin glass perspective on ferroic glasses. *Phys. Status Solidi* **251**, 1967 (2014).
[18] A. A. Bokov, M. Maglione, and Z.-G. Ye, Quasi-ferroelectric state in Ba ($Ti_{1-x}Zr_x$) O3 relaxor: dielectric spectroscopy evidence. *J. Phys.: Condens. Matter* **19**, 092001 (2007).
[19] S. A. Gridnev, A. A. Glazunov, and A. N. Tsotsorin, Nonlinear dielectric response of relaxor PMN-PZT ceramics under dc electric field. *Ferroelectrics*, **307**, 151 (2004).
[20] A. A. Bokov and Z.-G. Ye, Double freezing of dielectric response in relaxor Pb ($Mg_{1/3}Nb_{2/3}$)O_3 crystals. *Phys. Rev. B* **74**, 132102 (2006).
[21] H. N. Tailor, A. A. Bokov, Z. G. Ye, Freezing of polarization dynamics in relaxor ferroelectric $(1-x)$Pb($Mg_{1/3}Nb_{2/3}$)O_3–xBi($Zn_{1/2}Ti_{1/2}$)O_3 solid solution. *Curr. Appl. Phys.* **11**, 175 (2011).
[22] A. Dixit, S. B. Majumder, R. S. Katiyar, A. S. Bhalla, Studies on the relaxor behavior of sol-gel derived Ba(Zr_xTi_{1-x})O_3 ($0.30 \leq x \leq 0.70$) thin films. *J. Mater. Sci.* **41**, 87 (2006).
[23] A. K. Tagantsev, A. E. Glazounov, Does freezing in Pb($Mg_{1/3}Nb_{2/3}$)O_3 relaxor manifest itself in nonlinear dielectric susceptibility? *Appl. Phys. Lett.* **74**, 1910 (1999).
[24] J. P. Sethna, Entropy, Order Parameter, and Complexity. (Clarendon Press, Oxford, 2010).
[25] L. Cross. Relaxor ferroelectrics. *Ferroelectrics*, **76**,(1987).
[26] A. K. Josnscher, Universal relaxation law (Chelesea Dielectrics Press, 1996).
[27] A. K. Jonscher, Dielectric relaxation in solids (Chelesea Dielectrics Press, 1983).
[28] G. A. Smolenskii, Physical phenomena in ferroelectrics with diffused phase transition. *J. Phys. Soc. Jpn*. **28**, 26 (1970).
[29] V. V. Kirillov, V. A. Isupov, Relaxation polarization of $PbMg_{1/3}Nb_{2/3}O_3$ (PMN)-A ferroelectric with a diffused phase transition. *Ferroelectrics* **5**, 3 (1973).
[30] K. Uchino, S. Nomura, Critical exponents of the dielectric constants in diffused-phase-transition crystals. *Ferroelectrics* **44**, 55 (1982).
[31] R. Clarke and J. C. Burfoot, The diffuse phase transition in potassium strontium niobate. *Ferroelectrics*, **8**, 505 (1974).
[32] I. A. Santos, J. A. Eiras, Phenomenological description of the diffuse phase transition in ferroelectrics. *J. Phys. Condens. Matter* **13**, 11733 (2001).
[33] D. Wang and Z. Jiang, Dielectric response of $BaZrO_3$/$BaTiO_3$ superlattice, *J. Adv. Dielectr* **6**, 1650015 (2016).
[34] A. A. Bokov, I. P. Raevskii, and V. G. Smotrakov, Composition, ferroelectric and antiferroelectric ordering in Pb_2InNbO_6 crystals. *Sov. Phys. Sol. Stat.* **26**, 1708 (1984).
[35] N. Setter and L. Cross, The role of B-site cation disorder in diffuse phase transition behavior of perovskite ferroelectrics. *J. Appl. Phys.* **51**, 4356 (1980).
[36] N. Nakanishi, A. Nagasawa, Y. Murakami, Lattice stability and soft modes. *J. Phys. Colloques* **43**, 35 (1982).
[37] A. Bussmann-Holder, A. R. Bishop, T. Egami, Relaxor ferroelectrics and intrinsic inhomogeneity. *Europhys. Lett*. **71**, 249 (2005).
[38] W. Zhong, D. Vanderbilt, K. M. Rabe, Phase Transitions in $BaTiO_3$ from First Principles. *Phys. Rev. Lett.* **73**, 1861 (1994).
[39] W. Zhong, D. Vanderbilt, K. M. Rabe, First-principles theory of ferroelectric phase transitions for perovskites: the case of $BaTiO_3$. *Phys. Rev. B* **52**, 6301 (1995).
[40] R. A. Cowley, Structural phase transitions I. Landau theory. *Adv. Phys.* **29**, 1 (1980).
[41] A. Al-Barakaty, S. Prosandeev, D. Wang, B. Dhkil, and L. Bellaiche, Finite-temperature properties of the relaxor $PbMg_{1/3}Nb_{2/3}O_3$ from atomistic simulations. *Phys. Rev. B* **91**, 214117 (2015).
[42] D. Phelan, C. Stocka, J. A. Rodriguez-Riveraa, S. Chia, J. Leãoa , X. Long, Y. Xie, A. A. Bokov, Z.-G. Ye, P. Ganeshe, and P. M. Gehring, Role of random electric fields in relaxors, *PNAS* **111**, 1754 (2014).
[43] J. Hlinka, S. Kamba, J. Petzelt, J. Kulda, C. A. Randall, S. J. Zhang, Origin of the "Waterfall" Effect in Phonon Dispersion of Relaxor Perovskites. *Phys. Rev. Lett.* **91**, 107602 (2003).
[44] P. M. Gehring, S.-E. Park, and G. Shirane, Soft phonon anomalies in the relaxor ferroelectric $Pb(Zr_{1/3}Nb_{2/3})_{0.92}Ti_{0.08}O_3$. *Phys. Rev. Lett.* **84**, 5216 (2000).
[45] W. Kleemann, Cluster glass ground state via random fields and random bonds. *Phys. Status Solidi* **251**, 1993 (2014). .
[46] S. Prosandeev, D. Wang, A. R. Akbarzadeh, L. Bellaiche, First-principles-based effective Hamiltonian simulations of bulks and films made of lead-free Ba(Zr,Ti)O_3 relaxor ferroelectrics. *J. Phys . Condens. Matter*. **27**, 223202 (2015).
[47] S. O. Kasap, Principles of Electronic Materials and Devices, Third Edition (McGraw-Hill, 2006), pp612.
[48] We also verified that replacing the Langevin function with the simpler Curie law ($\sim 1/T$) will result in similar fitting results and analysis.
[49] R. Sommer, N. K. Yushin, J. J. Van Der klink. Dielectric susceptibility of PMN under DC bias. *Ferroelectrics* **127**, 235(1992).
[50] We have also found that relation between θ and frequency, f, follows the Vogel-Fulcher law, which indicates that there might be some connection between θ and T_m.
[51] I. K. Jeong, T. W. Darling, J. K. Lee, T. Proffen, R. H. Heffner, Direct observation of the formation of polar nanoregions in Pb($Mg_{1/3}Nb_{2/3}$)O_3 using neutron pair distribution function analysis. *Phys. Rev. Lett.* **94**, 147602 (2005).
[52] Y. Kuroiwa, S. Aoyagi, A. Sawada, J. Harada, E. Nishibori, M. Takata, M. Sakata, Evidence for Pb-O covalency in tetragonal $PbTiO_3$. *Phys. Rev. Lett.* **87**, 217601 (2001).
[53] I. A. Kornev, L. Bellaiche, P. E. Janolin, B. Dkhil, and E. Suard, Phase diagram of Pb(Zr,Ti)O_3 solid solutions from first principles. *Phys. Rev. Lett.* **97**, 157601 (2006).
[54] D. Sichuga and L. Bellaiche, Epitaxial Pb(Zr,Ti)O_3 ultrathin films under open-circuit electrical boundary conditions. *Phys. Rev. Lett*. **106**, 196102 (2011).
[55] Z. Jiang, R. Zhang, D. Wang, D. Sichuga, C.-L. Jia, and L. Bellaich, Strain-induced control of domain wall morphology in ultrathin $PbTiO_3$ films. *Phys. Rev. B* **89**, 214113 (2014).
[56] R. Pirc and R. Blinc, Vogel-Fulcher freezing in relaxor ferroelectrics. *Phys. Rev. B* **76**, 020101 (2007).
[57] W. Chen, Z.-G. Ye, Top seeded solution growth and characterization of piezo-/ferroelectric (1-x)Pb($Zn_{1/3}Nb_{2/3}$)O_3-$x$$PbTiO_3$single crystals, *J. Cryst. Growth* **233**, 503 (2001).
[58] D. La-Orauttapong, B. Noheda, Z.-G. Ye, P. M. Gehring, J. Toulouse, D. E. Cox, and G. Shirane, Phase diagram of the re-

laxor ferroelectric (1-x)Pb($Zn_{1/3}Nb_{2/3}$)O_3-$x$$PbTiO_3$, *Phys. Rev. B* **65**, 144101 (2002).

[59] The 0.87PZN-0.13PT data and fitting refer to its low temperature dielectric peak showing relaxor signatures.

[60] J. M. Valverde, On the negative activation energy for limestone calcination at high temperatures nearby equilibrium. *Chem. Eng. Sci.* **132**, 169 (2015).

[61] A. K. Jonscher, A new understanding of the dielectric relaxation of solids. *J. Mater. Sci.* **16**, 2037 (1981).